苏州大学推荐优秀应届本科毕业生免试攻读硕士学位研究生申请表

<table>
<tr><td>学号</td><td>1609404117</td><td>姓名</td><td colspan="2">余娉儿</td><td>性别</td><td colspan="2">女</td></tr>
<tr><td>出生日期</td><td colspan="2">1998.09.21</td><td>民族</td><td>汉族</td><td>政治面貌</td><td colspan="2">共青团员</td></tr>
<tr><td>学院</td><td colspan="3">材料与化学化工学部</td><td>专业</td><td colspan="2">材料科学与工程（工程强化）</td></tr>
<tr><td>手机</td><td colspan="3">15946801723</td><td>电子信箱</td><td colspan="2">yu1013556919@qq.com</td></tr>
<tr><td>违法违纪受处分者所受处分是否已撤销</td><td>是□
否□</td><td>已获学分数</td><td>142</td><td>公共外语课程平均学分绩点</td><td>3.7</td><td>大学外语等级考试成绩</td><td>雅思 6.5
六级 563
四级 536</td></tr>
<tr><td>平均学分绩点（GPA ）</td><td>3.5</td><td colspan="2">记等级的课程是否达 C 及以上</td><td>是□
否□</td><td colspan="2">体育保健班学生的体育课程是否达 D 等</td><td>是□
否□</td></tr>
<tr><td colspan="4">已修课程的学分绩点是否均达 1.0 及以上</td><td>是 ☑
否□</td><td colspan="2">申请时必修课成绩有无“弃考”标注</td><td>有□
无☑</td></tr>
<tr><td>何时受过
何种奖励</td><td colspan="7">苏州大学学习优秀奖学金二等奖学金（2018.12）
苏州大学第十九届“挑战杯”大学生课外学术科技作品竞赛三等奖（2018.12）
苏州大学第二十批课外学术科研基金重点项目结题优秀（主持人）（2018.11）
苏州大学学习优秀奖学金二等奖学金（2017.12）
苏州大学第十八届“挑战杯”大学生课外学术科技作品竞赛三等奖（2017.12）
苏州大学学部优秀共青团员（2019.03）
苏州大学“精神文明”专项奖（2018.12）
苏州大学材料与化学化工学部“暑期社会实践成果展示大赛”优秀奖（2018.10）
苏州大学材料与化学化工学部第一、二季度校园诺贝尔风云人物“志愿服务奖”（2018.06）
苏州大学材料与化学化工学部学生事务所“创赢”大赛三等奖（2018.04）
苏州大学“惠寒”支教课程设计大赛三等奖（2017.11）
苏州大学“优秀新生研讨课助教”（2017.06）
苏州大学材料与化学化工学部配音大赛优秀奖（2017.4）
苏州大学材料与化学化工学部新生英语短剧大赛二等奖（2016.11）</td></tr>
<tr><td>何时受过何种处分及撤销日期</td><td colspan="7">无</td></tr>
</table>

<table>
<tr><td>参加哪些科研工作，有何学术论文或著（译）作</td><td>2017.9-2018.9 在吴张雄老师课题组进行校级课外学术科研基金重点项目（TiO_2光催化降解染料研究）主持人，项目结题评为优秀
2018.10-至今 在杜玉扣老师课题组进行电催化剂性能研究(合成 PdCu 合金催化剂用于乙醇的电催化氧化反应）并撰写文章，文章已发表
1.<u>Ping’er Yu</u>, Hui Xu, Liujun Jin, Chunyan Chen, Hongyuan Shang, Qingyun Liu, Yukou Du. A novel catalyst for efficient electrooxidation of ethanol enabled by 3D open-structured PdCu nanocages, Journal of Colloid and Interface Science. 555 (2019) 195-202（第一作者）
2.Tongxin Song, Fei Gao, Yangping Zhang, <u>Ping’er Yu</u>, Chen Wang, Yukihide Shiraishi, Shujin Li, Caiqin Wang, Jun Guo , Yukou Du. Shape-controlled PdSn alloy as superior electrocatalysts for alcohol oxidation reactions, Journal of the Taiwan Institute of Chemical Engineers. 101 (2019) 167–176 （第四作者）

（申请学术特长生者还需填写：本人申请符合特长生申请条件的第<u>　　三　　</u>条）</td></tr>
<tr><td colspan="2">以上各项均由申请人本人如实填写。

申请人签名：

年　月　日</td></tr>
<tr><td rowspan="2">学院（部）</td><td>该生推免综合考核成绩
（含 GPA 成绩）</td><td></td><td>参与推免考核的所有学生数
（请注明按学院或按专业统计）</td><td></td></tr>
<tr><td>该生在参与推免排名全体学生中的综合测评名次
（请注明按学院或按专业统计）</td><td colspan="3"></td></tr>
</table>

考核及推荐意见	推荐意见： 学院（部）推免生遴选工作分管领导签字： 学院（部）盖章： 年　　月　　日

注：1、本表用 A4 纸正、反双面打印；

2、申请人须同时附成绩单和相关证明材料.

推荐信

被推荐人姓名:余娉儿

推荐老师：	杜玉扣	性别：	男
院系：	材料与化学化工学部	职称：	教授、博士生导师
Email：	duyk@suda. edu. cn	电话：	+86-13776101197
与学生关系：	导师☑ 班主任☐ 任课教师☐ 同课题组☑		

推荐意见：

余娉儿同学去年 9 月来我的课题组做实验，从事乙醇电催化性能研究的课题。她学习刻苦，经常学习到很晚回去。而且还热爱科研，平时看到她总是在实验室。寒假期间她留校做了一段时间实验才回家，并且开学也提前来实验室做实验研究。遇到问题，她积极找我讨论，然后再进行后续的实验。

在阅读了大量的文献之后，她参与她师姐的实验，并且作为 4 作参与撰写了一篇 sci 文章，目前已经发表。(Tongxin Song, Fei Gao, Yangping Zhang, ***Ping'er Yu***, Cheng Wang, Yukihide Shiraishi Yukihide, Shujin Li, Caiqin Wang, Jun Guo, Yukou Du, Journal of the Taiwan Institute of Chemical Engineers 101 (2019)167–176)

与此同时，她自己的实验（探究发现最合适的 Pd 和 Cu 的配比来得到最高效的催化性能）也比较顺利，在获得比较好的电催化活性和比较好的形貌之后，她开始向师兄学习处理数据，然后再进一步学习论文写作。最终经过不断的修改，文章在 8 月份初正式发表（***Ping'er Yu***, Hui Xu, Liujun Jin, Chunyan Chen, Hongyuan Shang, Qingyun Liu, Yukou Du. A novel catalyst for efficient electrooxidation of ethanol enabled by 3D open-structured PdCu nanocages, Journal of Colloid and Interface Science. 555 (2019) 195-202）在实验的过程中，她掌握了加热法制备 Pd-Cu 的纳米笼，以及其用于电催化乙醇的实验测试，熟练学会了对催化剂进行循环伏安（CV）、电化学阻抗（EIS）、时间电流（I-t）等测试的技能， 也学习并实践基本表征方法例如 X 射线衍射（XRD）、SEM、TEM、X 射线光电子能谱分析（ XPS）等，科研论文撰写的能力也得到了锻炼。

因此，我认为她掌握了足够的专业知识能力和操作能力，能够通过推免并且进入研究生阶段完成相应的课程和科研任务。

推荐人签名：杜玉扣 2019 年 9 月 9 日

推荐信

被推荐人姓名:余娉儿

推荐老师:	吴张雄	性别:	男
院系:	材料与化学化工学部	职称:	教授、博士生导师
Email:	zhangwu@suda.edu.cn	电话:	0512-65882782
与学生关系:	导师☐ 班主任☐	任课教师☑	同课题组☐

推荐意见:

大学一年级第一学期，我是余娉儿同学《大学化学》的任课老师。该生很上进，上课认真，自主学习能力较强，善于沟通，发现问题后能及时通过查阅资料与咨询老师和同学，寻求解决的方法。

大二到大三年级，余同学抽取部分课余时间，在我课题组做实验，并申请获批了苏州大学第二十批的本科生科研项目，开展关于多孔二氧化钛颗粒的制备与光催化工作。该生主观能动性较强，在组期间，能自觉阅读了英文文献，并积极思考，形成自己的想法，并提出不同的或改进的方法。通过与其数次讨论课题研究内容与实验进展，该生表现出了清晰的逻辑思维，求知欲高，可塑性强，具有良好的学术研究潜质。在组期间，她初步学习了 X 射线衍射（XRD）、SEM、热重分析（TG）、总有机碳分析（TOC）、紫外-可见光谱(UV-Vis)等的先进设备的工作原理，并学会了设备的基本的常规操作方法。其课题进展良好，项目顺利结题，最终取得了结项优秀的成绩。该生是一位容易相处、且乐于助人，在实验室期间，她和课题组成员相处很好，具有良好的协作精神。

此外，该生还是学部学生事务所的部长，具有较强的领导能力，平时与学部学生们的相处很融洽，是一位科研能力和交际能力兼备的优秀学生。

因此，我非常高兴推荐该生参加推免，我相信她有能力在研究生阶段表现得优秀，并相信她能在将来的深造中能取得优秀的成绩。

推荐人签名：2019年9月10日

推荐信

被推荐人姓名:余娉儿

推荐老师：	周祎	性别	女
院系：	材料与化学化工学部	职称：	教授、硕士生导师
Email：	yizhou@suda.edu.cn	电话	+86-0512-65882653
与学生关系：	导师□ 班主任□ 任课教师 ☑ 同课题组□		

推荐意见：

余娉儿同学是我在 2017-2018 学年上学期教授的专业必修课《材料科学与工程导论》上的一名学生。我对她印象很深刻，因为她总是坐在第一排，学习刻苦上课认真听讲，下课积极提问，并在学期末取得了这门课程的良好成绩。

在课程当中她总能够问出一些比较有意思的问题，例如如何才能做出纳米级别的刀，在切西瓜的时候不会有汁水留下来；蚊子的尸体含有彩色的光这是一种什么材料？下课后她也会向我探讨一些关于大学期间的学习生活和今后职业规划的一些问题，还会讨论目前的研究热点，本科生发文章的要求和以后未来攻读博士研究生还是参加工作等话题。我觉得她是一个很有想法的学生。

在课程当中有一环节需要同学们作 PPT 演讲，题目是大家自己定的，余娉儿同学选的主题是关于光催化的研究课题。她主要介绍了光催化的两部分应用，一个是关于环境保护方面的，她结合当时自己在课题组的研究进展情况，清晰地讲述了二氧化钛降解染料废水的研究和应用。另一个是关于能源利用方面的，她讲到了目前最热的钙钛矿电池，以及目前的一些突破和难点所在，整个演讲的过程很流畅，对于同学们提出来的问题也做了很好的解答。我看的出来她查了很多资料，也做了非常充分的准备。

我认为她有足够的学习和掌握新知识的能力、具有创新的思想和严谨的科学素养，有能力完成将来研究生阶段的课程和科研任务。

推荐人签名：周祎 2019年 9月 10日

苏州大学学生成绩单

姓名:余婷儿　　学号:1609404117　　学院(部):材料与化学化工学部　　专业:材料科学与工程（工程强化）　　层次:本科　　学制:四年

课　程	课程性质	成绩	学分	绩点
2016-2017学年第一学期				
生物摄影与作品赏析	通识选修课程	91	2.0	3.8
中国地方文化英语教学	通识选修课程	89	2.0	3.8
大学英语（一）	公共基础课程	88	4.0	3.7
高等数学（一）上	公共基础课程	90	5.0	3.8
公共体育（一）	公共基础课程	B	1.0	-
计算机信息技术 I	公共基础课程	78	3.0	3.1
军事技能	公共基础课程	A	1.0	-
形势与政策	公共基础课程	A	2.0	-
英语听说（一）	公共基础课程	88	0.0	3.7
英语写作（一）	公共基础课程	89	0.0	3.8
职业生涯规划指导（上）	公共基础课程	A	0.5	-
大学化学*	大类基础课程	79	4.0	3.2
工程制图（双语）*	大类基础课程	83	3.0	3.5
化学工程导论*	大类基础课程	83	2.0	3.5
2016-2017学年第二学期				
大学生大学生涯设计	新生研讨课程	94	1.0	3.9
VB程序设计	公共基础课程	78	4.0	3.1
大学英语（二）	公共基础课程	87	2.0	3.7
高等数学（一）下	公共基础课程	'82	5.0	3.4
公共体育（二）	公共基础课程	B	1.0	-
普通物理（二）（上）	公共基础课程	91	4.0	3.8
英语听说（二）	公共基础课程	89	0.0	3.8
英语写作（二）	公共基础课程	90	0.0	3.8
大学化学实验*	大类基础课程	90	1.5	3.8
工程数学（双语）	专业必修课程	84	4.0	3.5
数值建模与分析	专业必修课程	60	2.0	1.0
纳米世界	公共选修课程	C	2.0	-
2017-2018学年第一学期				
人与自然的终极奥秘	通识选修课程	95	2.0	4.0
吴文化史专题（网络）	通识选修课程	93	2.0	3.9
中外优秀合唱作品欣赏及实践	通识选修课程	95	2.0	4.0
大学英语（三）	公共基础课程	88	2.0	3.7
公共体育（三）	公共基础课程	B	1.0	-
普通物理（二）（下）	公共基础课程	85	4.0	3.6
普通物理实验	公共基础课程	89	1.0	3.8
中国近现代史纲要	公共基础课程	A	2.0	-
电工电子学	大类基础课程	94	2.0	3.9
有机化学（二）（上）*	大类基础课程	87	3.0	3.7
材料科学与工程导论	专业必修课程	82	3.0	3.4
环境工程导论	专业必修课程	88	2.0	3.7
2017-2018学年第二学期				
大学英语（四）	公共基础课程	90	2.0	3.8
公共体育（四）	公共基础课程	C	1.0	-
军事理论	公共基础课程	B	2.0	-
毛泽东思想和中国特色社会主义理论体系概论社会实践（上）	公共基础课程	A	1.0	-
思想道德修养与法律基础	公共基础课程	B	3.0	-
物理化学（二）（上）*	大类基础课程	80	3.0	3.3
有机化学（二）（下）*	大类基础课程	85	3.0	3.6
有机化学实验(二)*	大类基础课程	91	2.0	3.8
化工原理（一）*	专业必修课程	71	2.0	2.4
金工实习	专业必修课程	86	2.0	3.6
光电材料与器件基础	专业选修课程	90	2.0	3.8
2018-2019学年第一学期				
毛泽东思想和中国特色社会主义理论体系概论	公共基础课程	D	4.0	-
物理化学（二）（下）*	大类基础课程	91	3.0	3.8
物理化学实验（二）*	大类基础课程	82	1.5	3.4
化工热力学基础*	专业必修课程	74	3.0	2.7
化工原理（二）*	专业必修课程	87	2.0	3.7
化工原理实验*	专业必修课程	80	2.0	3.3
材料化学	专业选修课程	86	2.0	3.6
创新创业实践（一）	专业选修课程	90	2.0	3.8
核磁共振波谱学基础	专业选修课程	84	2.0	3.5
绿色化学	专业选修课程	90	2.0	3.8
纳米生物技术	专业选修课程	90	2.0	3.8
2018-2019学年第二学期				
健康标准测试（一）	公共基础课程	C	0.0	-
马克思主义基本原理	公共基础课程	A	3.0	-
职业生涯规划指导（下）	公共基础课程	C	0.5	-
反应工程实验*	专业必修课程	95	2.0	4.0
化学反应工程*	专业必修课程	89	2.0	3.8
颗粒科学与技术*	专业必修课程	86	2.0	3.6
创新创业实践（二）	专业选修课程	90	2.0	3.8
以下空白				

已修总学分：　142　　平均学分绩点(GPA)：　3.5

苏州大学教务部　2019/9/4

备注：1. 课程名称标注“*”的课程为学位课程；2. 课程名称标注“#”的课程成绩为重修成绩；3. 课程性质为“其他课程”的或以等级形式记录的课程成绩不计算绩点，且不计入平均学分绩点(GPA)，等级A、B、C、D、F分别对应优秀、良好、中等、及格和不及格；4. 以百分制形式记录的课程成绩绩点是基于4分制，其具体计算公式如下(其中S为以百分制记录的成绩)：绩点=4-3×(100-S)²/1600 (60≤S≤100)，绩点=0 (S<60)；5. 平均学分绩点(GPA)=Σ(学分×绩点)/Σ学分（学分不包括以“其他课程”学分及等级形式记录的课程学分）。

Journal of Colloid and Interface Science 555 (2019) 195–202

Contents lists available at ScienceDirect

Journal of Colloid and Interface Science

journal homepage: www.elsevier.com/locate/jcis

Regular Article

A novel catalyst for efficient electrooxidation of ethanol enabled by 3D open-structured PdCu nanocages

Ping'er Yu [a], Hui Xu [a], Liujun Jin [a], Chunyan Chen [a], Hongyuan Shang [a], Qingyun Liu [b,*], Yukou Du [a,*]

[a] College of Chemistry, Chemical Engineering and Materials Science, Soochow University, Suzhou 215123, PR China
[b] College of Chemical and Environmental Engineering, Shandong University of Science and Technology, Qingdao 266590, PR China

GRAPHICAL ABSTRACT

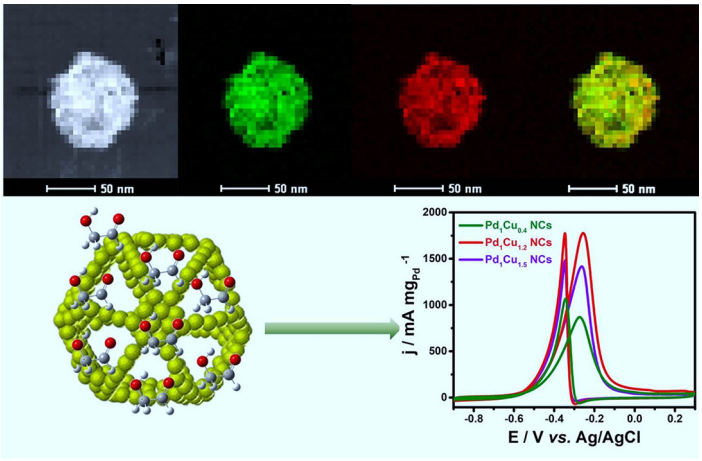

ARTICLE INFO

Article history:
Received 21 June 2019
Revised 27 July 2019
Accepted 29 July 2019
Available online 30 July 2019

Keywords:
PdCu
Ethanol oxidation reaction
Electrocatalysts
Highly open nanocages

ABSTRACT

Mastery over the structure at nanoscale can efficiently tune the catalytic properties of catalysts, enabling great enhancement in electrocatalytic performance toward liquid fuel electrooxidation reactions. Herein, we demonstrate a facile one-pot method for the successful fabrication of binary PdCu nanocatalysts bounded with 3D open-structured nanocages, which show the advantages of high surface areas, facile mass/electron transport, and strong synergistic effect. Impressively, the resultant 3D open-structured PdCu nanocages (NCs) show large promotion in electrocatalytic performance toward ethanol oxidation reaction (EOR) with the mass activity of 1790.8 mA mg^{-1}, being 3.3 times higher than that of commercial Pd/C (536.2 mA mg^{-1}). Besides, the specific activity for EOR on PdCu NCs (7.7 mA cm^{-2}) is also comparable to many Pt-based electrocatalysts, suggesting the dramatically improved electrocatalytic activity. The outstanding electrocatalytic performance of binary PdCu catalysts is attributed to the highly open 3D nanocage structure and strong electronic effect of Pd and Cu.

1. Introduction

Ethanol, with many overriding virtues, such as high theoretical energy density, low toxicity, and abundant availability, has been

* Corresponding authors.
E-mail addresses: qyliu@sdust.edu.cn (Q. Liu), duyk@suda.edu.cn (Y. Du).

https://doi.org/10.1016/j.jcis.2019.07.092
0021-9797/

generally regarded as the desirable energy sources for fuel cell technology [1,2]. Consequently, direct ethanol fuel cells (DEFCs) have received increasing notices based on fossil fuel combustion for portable power generation. Unfortunately, the sluggish reaction kinetic on anodic ethanol oxidation reaction (EOR) has restricted their commercial application. To boost the practical application of DEFCs [3,4], it is necessary to improve the ability of catalysts to promote the anodic reaction kinetics.

At present, platinum (Pt) is generally regarded as the most efficient material for electrocatalytic reactions, while its high cost, limited natural reserve, and weak ability for splitting C—C bonds of ethanol badly hindered its large-scale applications [5–7].To address this issue, exploring appropriate material to substitute noble Pt is urgently sought. Recently, palladium (Pd) has been developed and employed as ideal substitute of Pt due to its Pt-like properties but relatively low cost [8,9]. While, the monometal Pd with limited active sites and poor stability have seriously hampered its practical application, resulting in unsatisfactory electrocatalytic performance [10,11]. Update, many efficient strategies have been developed by previous researchers. On the one hand, incorporating the second metal into Pd to generate the Pd-based alloy nanocatalysts has been widely considered as one of the most feasible approaches to obtain desirable anode electrocatalysts because of the generated two effects (electronic effect and synergistic effects between Pd and Cu) [12,13], which not only cut down the cost of catalyst, but also largely promote the electrocatalytic performances of catalysts. For example, the introduction of Cu facilitates the formation of OH species [14,15], which are favorable for improving the antipoisoning capability of catalysts, leading to the large promotion of electrocatalytic performances.

Apart from the composition influences, the morphology and architecture of catalysts can also strongly affect their electrocatalytic performance due to the geometric effect derived from lattice strain [16–18]. Moreover, the catalysts with high active areas can also expose more surface active sites available for liquid fuel, leading to the great enhancement in electrocatalytic activity and durability. For instance, the highly open 3D nanocages commonly show excellent electrocatalytic performance toward liquid fuel oxidation reaction due to their abundant merits, such as rich active sites, facilitated mass/electron transfer, and abundant holes [19,20]. Although these beneficial terms, the approaches for the synthesis of highly open 3D nanocages are commonly complicated, which often take two or more steps [21,22]. Therefore, it will be meaningful to synthesize nano-caged catalysts through a simple method.

Taking into account the advantages of chemical composition and structure, herein, we demonstrated the synthesis of porous PdCu nanocages through a facile one-pot wet-chemical method employing $Fe(Ac)_2$ as the structure-directing agent. Owing to the bifunctional effect and geometric effect, the optimized PdCu NCs showed excellent electrocatalytic activity for EOR. More importantly, the resultant PdCu NCs could also maintain high activity for long-term electrochemical tests, exhibiting a novel class of efficient anode catalysts for DEFCs.

2. Experimental section

2.1. Chemicals

Copper (II) chloride, sodium tetrachloropalladate (Na_2PdCl_4), Nafion (5%), N,N-Dimethylformamide (DMF), and tungsten carbonyl ($W(CO)_6$) were purchased from Sigma-Aldrich. Acetic acid (CH_3COOH, AA) was purchased from Aladdin. Ethanol (C_2H_6O) and potassium hydroxide (KOH) were purchased from Sinopharm Chemical Reagent Co. Ltd. (Shanghai, China).

2.2. Synthesis of 3D open-structured PdCu NCs

The preparation of 3D open-structured PdCu NCs is based on our previous work. In the typical synthesis procedure, 10 mg of $CuCl_2$, 10 mg of Na_2PdCl_4, 50 mg of PVP, 30 mg of $W(CO)_6$, and 10 mg of $Fe(Ac)_2$ were dispersed into the solution containing 8.0 mL of DMF and 2.0 mL of acetic acid in a vial. After keeping sonicating for 10 min, the vial was then heated in an oil bath from room temperature to 150 °C and keeping reacting for 3 h. After cooling to room temperature, the products were then collected by sonicating and washing with ethanol for three times.

2.3. Characterizations

The morphologies of samples were analyzed by transmission electron microscope (TEM, FEI Tecnai G^2-20) and high-angle annular dark field-scanning transmission electron microscopy (HAADF-STEM). The chemical compositions of the samples were determined by elemental mappings, scanning electron microscope energy spectrometer (SEM-EDS), and X-ray photoelectron spectroscopy spectra (XPS). High-resolution TEM (HRTEM) and X-ray diffraction (XRD) were also performed to characterize the crystal structures of samples.

2.4. Electrochemical measurements

The EOR electrochemical measurements for 3D open-structured PdCu NCs were performed in a three-electrode system with CHI760e electrochemical workstation employing glassy carbon electrode (GCE) as working electrode, Ag/AgCl and Pt wire as reference and counter electrode, respectively. To improve the conductivity and specific areas of the as-obtained catalysts, the pre-prepared samples (2 mg) were first loaded on the surface of porous carbon materials (8 mg), then the mixture was dispersed into the 2 mL of solution containing isopropanol and Nafion (v/v = 1/0.005) under sonication. Finally, 5 μL of the catalyst dispersions were added dropwise on GCE surface and dried in air. The electrocatalytic activities of catalysts were evaluated by cyclic voltammetry (CV) at the scan rate of 50 mV s^{-1}. And the chronoamperometry (CA) and continuous CVs of 300 cycles were performed to evaluate the durability of electrocatalysts. The electrochemical impedance spectroscopy (EIS) conducted at the frequency ranging from 1 to 100,000 Hz was employed to evaluate the conductivity and reaction kinetic of catalysts.

3. Results and discussion

As illustrated by Fig. 1, the 3D open-structured PdCu NCs were synthesized through a facile one-pot method, where $CuCl_2$ and Na_2PdCl_4 as precursors, PVP as stabilizer, $W(CO)_6$ and $Fe(Ac)_2$ as structure-directing agents. The morphology and structure of the products can be characterized by TEM and XRD. Fig. 2a–c showed that the as-prepared $Pd_1Cu_{1.2}$ nanocrystals were well dispersed and featured with the typical 3D nanocage structure (Figs. S1 and

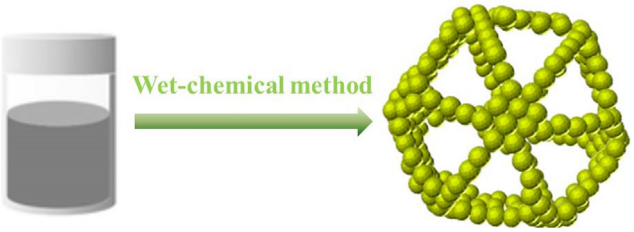

Fig. 1. Scheme illustration for the synthesis of 3D PdCu NCs.

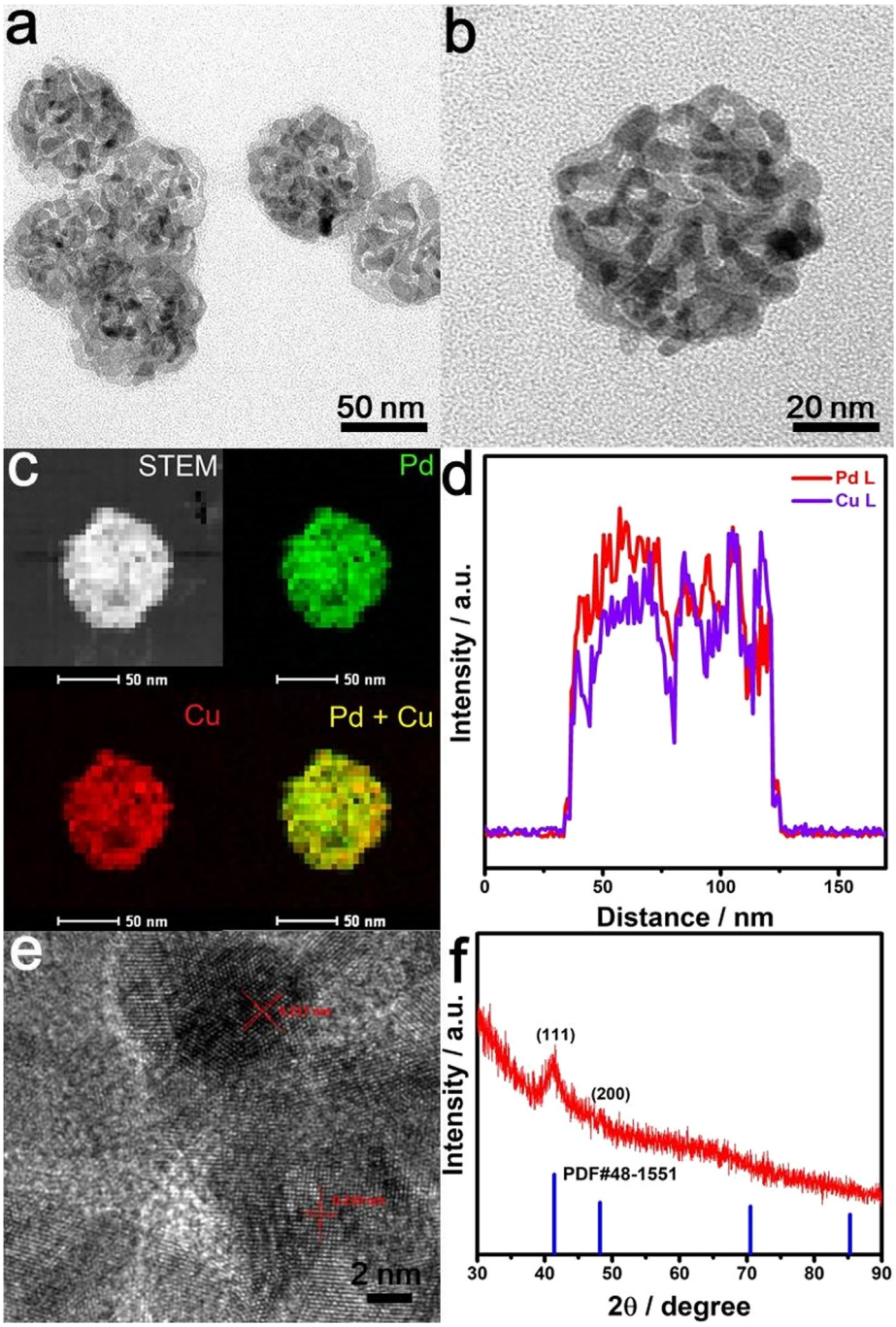

Fig. 2. (a, b) Representative TEM images of $Pd_1Cu_{1.2}$ NCs with different magnifications. (c) HAADF-STEM image, elemental mappings, and (d) compositional line profiles for $Pd_1Cu_{1.2}$ NCs. (e) HRTEM image and (f) XRD pattern of $Pd_1Cu_{1.2}$ NCs.

S2), where the chemical composition was analyzed by SEM-EDS (Fig. S3). The average particle size was calculated to be around 85 nm (Fig. S4). The chemical compositions have been analyzed by elemental mappings, and the corresponding elemental mapping images revealed that both Pd and Cu were uniformly distributed in the nanocage, clearly demonstrating the generation of PdCu nanocage (Fig. 2d). The results of compositional line profile data are consistent with the analysis of elemental mapping, further confirming the formation of PdCu nanocages. The HRTEM images have also been obtained to reveal the crystal structure of the PdCu nanocages. As seen in Fig. 2e, the clear lattice fringes with the interplanar spacing of 0.217 and 0.219 nm is corresponding to the (1 1 1) crystal plane of face-centered cubic PdCu alloy [23]. To further elucidate the crystal structure of such PdCu nanocages, the corresponding XRD patterns have also been obtained. As observed in Fig. 2f, the representative diffraction peaks at 41.4°, 48.2°, 70.5°, and 85.3° are well indexed to the (1 1 1), (2 0 0), (3 1 1), and (2 2 2) crystal facets of PdCu alloy (JCPDF#48-1551), respectively, further illustrating the formation of PdCu alloy[24].

The surface chemical compositions and electronic structures of $Pd_1Cu_{1.2}$ NCs were further analyzed by XPS. Fig. 3a showed the XPS survey scan of $Pd_1Cu_{1.2}$ NCs, where the representative peaks at the binding energy around 340 and 950 eV were corresponding to the Pd 3d and Cu 2p, respectively. Also, the Pd 3d spectrum exhibits peaks at 340.3 eV and 335.4 eV were corresponding to metallic Pd of Pd $3d_{3/2}$ and Pd $3d_{5/2}$, while the other two peaks at

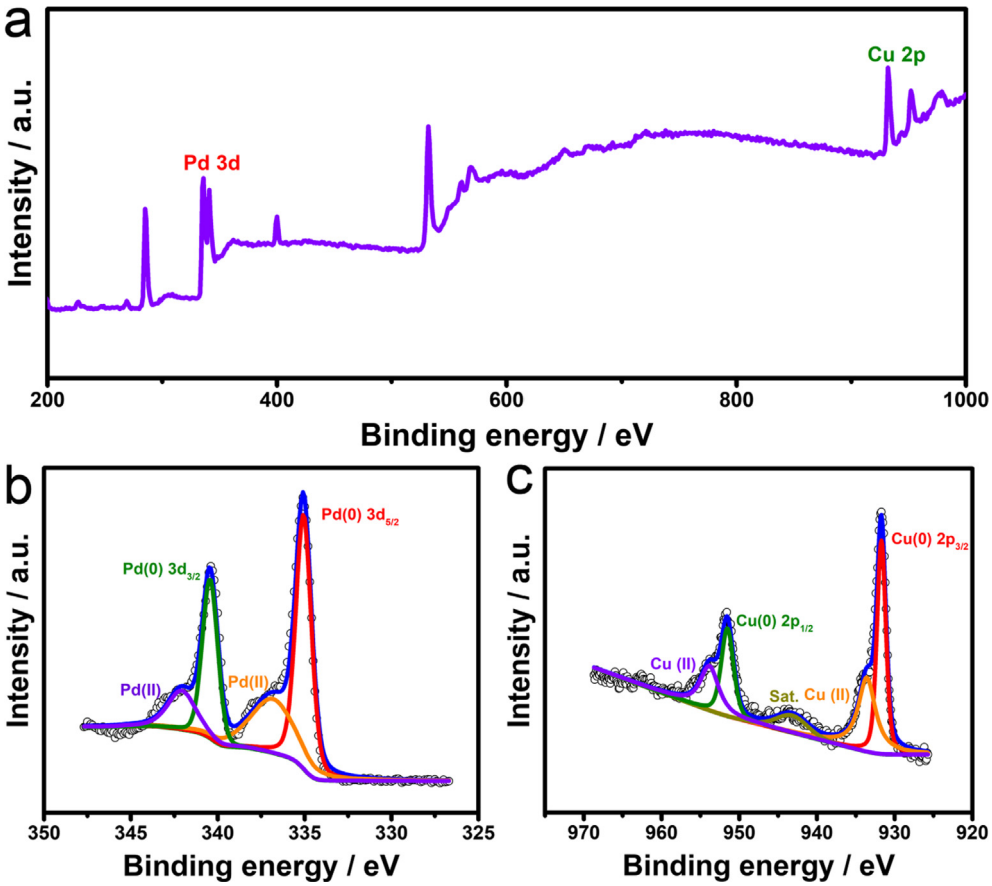

Fig. 3. (a) XPS spectra of survey scan of $Pd_1Cu_{1.2}$ NCs. High-resolution XPS spectra of (b) Pd 3d and (c) Cu 2p in 3D $Pd_1Cu_{1.2}$ NCs.

342.1 eV and 337.0 eV were ascribed to the Pd(II) of Pd $3d_{3/2}$ and Pd $3d_{5/2}$, respectively [25]. The peaks of Pd(0) were remarkably stronger than that of Pd(II), suggesting that most of Pd atoms have been reduced in this reaction environment [14]. Fig. 3c recorded the XPS spectrum of Cu 2p, where the peaks at 931.7 eV (Cu $2p_{3/2}$) and 951.6 eV (Cu $2p_{1/2}$) were the indicative of Cu(0), while the peaks at 933.7 eV and 953.9 eV were corresponding to the Cu (II) of Cu $2p_{3/2}$ and Cu $2p_{1/2}$, respectively [26]. These analyses have indicated that the main chemical compositions on the surface of PdCu NCs were metallic Pd and Cu, which were active to the small organic molecules [27].

To decode the formation mechanism of the 3D PdCu NCs, the controlled experiments regarding the reaction agents have been conducted. First, we have thoroughly investigated the role of $CuCl_2$ in the synthesis of 3D PdCu NCs. As seen in Fig. S5, the reaction in the absence of $CuCl_2$ while keeping other conditions the same yield some uniform Pd nanocages, which were similar to 3D PdCu NCs. Second, we have also thoroughly studied the influences of amounts of $CuCl_2$ for the synthesis of 3D PdCu NCs by tuning the amounts of $CuCl_2$ to 5 mg and 15 mg, the atomic ratios were 1:0.4 and 1:1.5, respectively, determined by SEM-EDS (Fig. S6). As displayed in Fig. 4a–d, both $Pd_1Cu_{0.4}$ and $Pd_1Cu_{1.5}$ also showed the typical 3D nanocage-like structure, which were similar to 3D $Pd_1Cu_{1.2}$ NCs. Moreover, the XRD diffraction peaks of both $Pd_1Cu_{0.4}$ and $Pd_1Cu_{1.5}$ NCs were well indexed to the fcc PdCu alloy (JCPDF#48-1551) (Fig. 4e and f), indicating the successful construction of PdCu alloy structure [28]. Moreover, we have also clearly researched the effects of PVP and $Fe(Ac)_2$ for the successful fabrication of nanocage-like PdCu electrocatalysts. Fig. S7 shows the representative TEM images of PdCu nanomaterials that prepared in the absence of PVP and $Fe(Ac)_2$ while keeping other conditions the same. From Fig. S7, it is clearly found that the PdCu are featured with the typical 3D nanoflowers that assembled by 2D nanosheets but not 3D nanocage structure, illustrating that the addition of PVP and $Fe(Ac)_2$ was essential to the successful syntheses of highly open 3D PdCu nanocages.

In consideration of the unique 3D open-structured nanocage structure and the strong alloy effect, such 3D open-structured PdCu nanocages are thus highly expected to serve as efficient anode electrocatalysts for EOR in fuel cells. To this end, we herein thoroughly evaluate their electrocatalytic performance towards EOR in alkaline media. For comparison, the electrocatalytic performance of $Pd_1Cu_{0.4}$ NCs, $Pd_1Cu_{1.5}$ NCs and commercial Pd/C catalysts have also been thoroughly investigated. Fig. 5a shows the CV of PdCu NCs with different atomic ratios in 1 M KOH solution, where the peak from −0.2 to 0 V in the forward scan is corresponding to the oxidation of Pd, while the peak from −0.2 to −0.4 V in the backward scan is relating to the reduction of Pd-O that formed in the forward scan. Taking into accounting that the charge during reduction of Pd-O into Pd is associated with the number of Pd atoms on the surface of catalysts [29]. Therefore, the electrochemically active surface areas (ECSAs) of different catalysts were calculated according to the Eq. (1)

$$ECSA = Q/(0.405 \times Pd_m) \quad (1)$$

The ECSAs calculated based on Eq. (1) are recorded in Fig. 5b, as seen, the ECSAs are 22.2, 23.2, and 22.5 $m^2\ g^{-1}$ for $Pd_1Cu_{0.4}$ NCs, $Pd_1Cu_{1.2}$ NCs, and $Pd_1Cu_{1.5}$ NCs, respectively. The high ECSA is favorable for exposing more surface active sites available for reactants, being beneficial for promoting the electrocatalytic performance. The electrocatalytic activities of $Pd_1Cu_{0.4}$ NCs, $Pd_1Cu_{1.2}$ NCs, and $Pd_1Cu_{1.5}$ NCs were tested by CV in 1 M KOH + 1 M

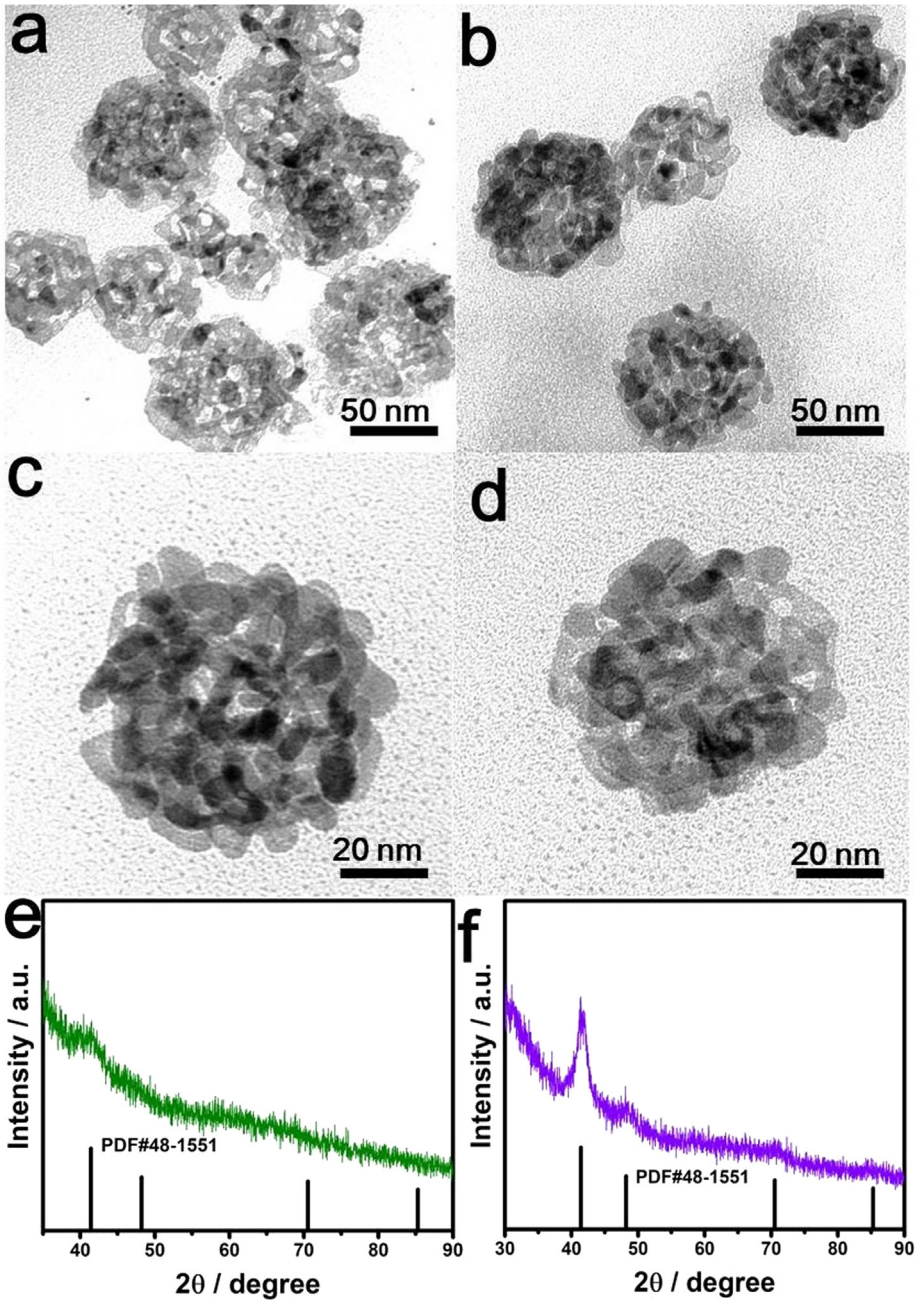

Fig. 4. TEM images of (a, c) $Pd_1Cu_{0.4}$ NCs and (b, d) $Pd_1Cu_{1.5}$ NCs with different magnifications. XRD patterns of (e) $Pd_1Cu_{0.4}$ NCs and (f) $Pd_1Cu_{1.5}$ NCs.

ethanol solution at the sweeping rate of 50 mV s^{-1}. For ease of comparison, the electrocatalytic activity of commercial Pd/C has also been evaluated. As seen in Fig. 5c, the forward peak at the potential around −0.3 V is associated with the oxidation of ethanol, while the other one in the backward scan is corresponding to the further oxidation of unremoved ethanol or intermediates [30]. The current densities were normalized to the mass of catalysts on the surface of GCE. In addition, the mass activities (normalized to the mass of Pd) and specific activities (normalized to the ECSA) of different catalysts have also been recorded in Fig. 5d. As seen, the $Pd_1Cu_{1.2}$ NCs showed the mass activity of 1790.8 mA mg^{-1}, which was 3.3 times higher than Pd/C (536.2 mA mg^{-1}) (Fig. S8), and being much higher than those of recently reported Pd-based nanocatalysts (Table S1). In addition, both of $Pd_1Cu_{0.4}$ NCs (881.7 mA mg^{-1}) and $Pd_1Cu_{1.5}$ NCs (1427.2 mA mg^{-1}) also displayed much higher mass activity than Pd/C, indicating the excellent electrocatalytic properties of 3D PdCu NCs. More importantly, all of the PdCu NCs also exhibited relatively high specific activity of 7.7 mA cm^{-2}, 6.3 mA cm^{-2}, and 4.0 mA cm^{-2} for $Pd_1Cu_{1.2}$ NCs, $Pd_1Cu_{0.4}$ NCs, and $Pd_1Cu_{1.5}$ NCs, respectively, further demonstrating the excellent electrocatalytic properties of 3D PdCu NCs. Considering their highly open 3D cage-like structural features, the enhanced electrocatalytic activities of PdCu NCs are attributed to their sufficient surface active sites from both interior and exterior surface [31–33]. Moreover, the introduction of Cu facilitates the adsorption of OH^- and OH_{ads}, benefiting for the enhancement of oxidation kinetics [34–38].

To further reveal the reason for the enhancement of electrocatalytic performance toward EOR, the conductivities of $Pd_1Cu_{0.4}$ NCs, $Pd_1Cu_{1.2}$ NCs, and $Pd_1Cu_{1.5}$ NCs were investigated by means of EIS

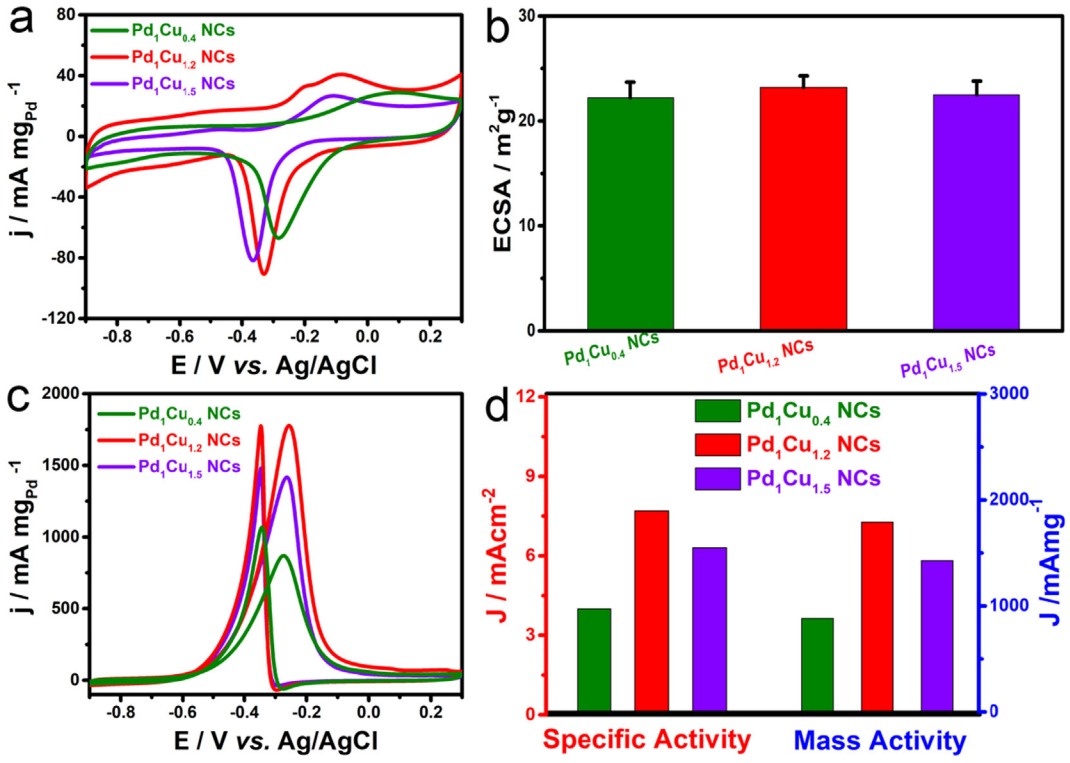

Fig. 5. CV curves of $Pd_1Cu_{0.4}$ NCs, $Pd_1Cu_{1.2}$ NCs, and $Pd_1Cu_{1.5}$ NCs in (a) 1 M KOH solution and (b) 1 M KOH + 1 M CH_3CH_2OH solution. (c) Corresponding histograms of ECSAs and (d) calculated electrocatalytic activities for $Pd_1Cu_{0.4}$ NCs, $Pd_1Cu_{1.2}$ NCs, and $Pd_1Cu_{1.5}$ NCs.

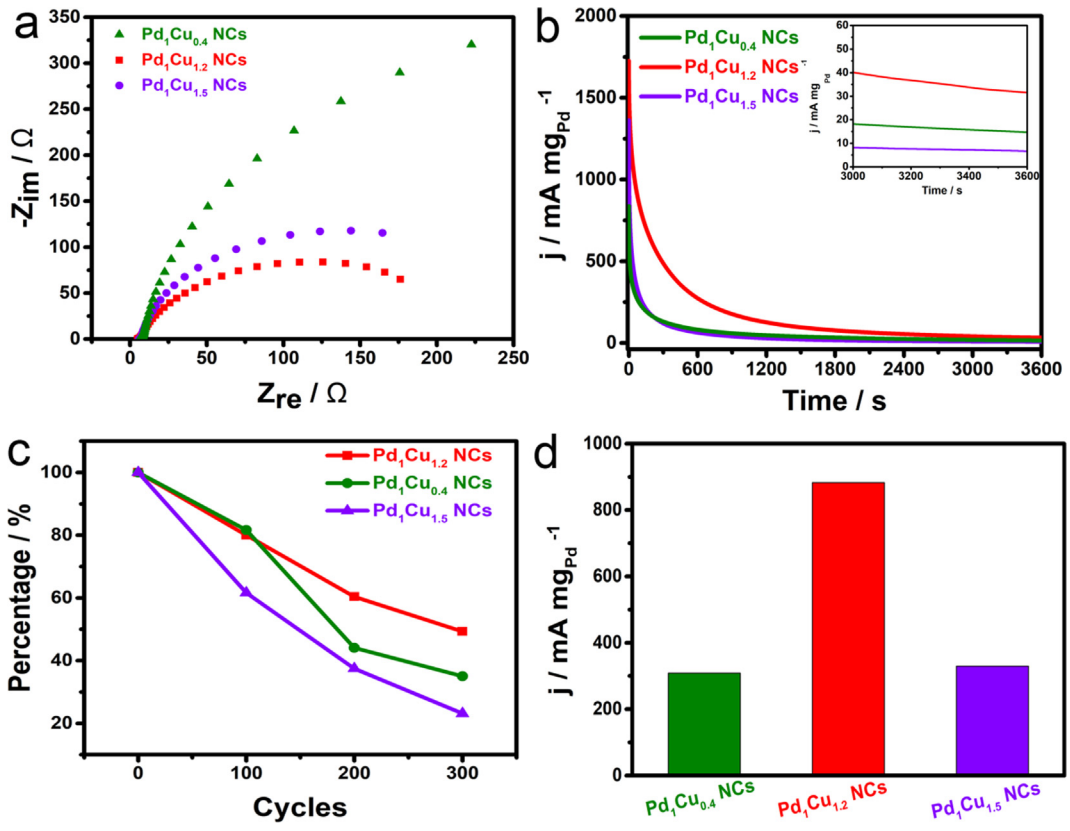

Fig. 6. (a) Nyquist plots and (b) CA curves of $Pd_1Cu_{0.4}$ NCs, $Pd_1Cu_{1.2}$ NCs, and $Pd_1Cu_{1.5}$ NCs in 1 M KOH + 1 M CH_3CH_2OH solution at the potential of −0.3 V. (c) Normalized current percentage of $Pd_1Cu_{0.4}$ NCs, $Pd_1Cu_{1.2}$ NCs, and $Pd_1Cu_{1.5}$ NCs versus cycles number in 1 M KOH + 1 M CH_3CH_2OH solution at the scan rate of 50 mV s^{-1}. (d) The retained mass activities of $Pd_1Cu_{0.4}$ NCs, $Pd_1Cu_{1.2}$ NCs, and $Pd_1Cu_{1.5}$ NCs after potential cycles of 300.

measurements. As seen in Fig. 6a, the composition-optimized $Pd_1Cu_{1.2}$ NCs showed the smallest diameter of the impedance arc (DIA), suggesting the smallest charge transfer resistance for the EOR in alkaline media, which can also account for the highest electrocatalytic activity of $Pd_1Cu_{1.2}$ NCs [39].

From the practical viewpoint, the long-term stability of catalyst is equally important to the activity. To this end, we herein also conducted a series of electrochemical tests to evaluate their long-term stabilities. Fig. 6b showed the CA curves of $Pd_1Cu_{0.4}$ NCs, $Pd_1Cu_{1.2}$ NCs, and $Pd_1Cu_{1.5}$ NCs at −0.3 V for 3600 s. As seen, the $Pd_1Cu_{1.2}$ NCs could retain the highest current density of 31.5 mA mg^{-1} among these electrocatalysts investigated. Besides, the continuous CVs of 300 cycles have also been conducted. Fig. 6c showed the electrochemical response of $Pd_1Cu_{0.4}$ NCs, $Pd_1Cu_{1.2}$ NCs, and $Pd_1Cu_{1.5}$ NCs after different numbers of potential cycles by CV. And the retained mass activity after 300 potential cycles have also been recorded in Fig. 6d. Surprisingly, although the successive CV of 300 cycles, the 3D PdCu NCs could maintain high normalized current percentage (normalized to the initial current density) and retained mass activity. Particularly for 3D $Pd_1Cu_{1.2}$ NCs, whose normalized current percentage and retained mass activity are as high as 49.3% and 882.8 mA mg^{-1}, respectively, much higher than those of commercial Pd/C catalysts (20.6% and 109.3 mA mg^{-1}) (Fig. S9). These results have further confirmed the outstanding long-term stability.

4. Conclusion

To summarize, the high-quality 3D open-structured PdCu NCs are constructed through a facile one-pot method by employing $Fe(Ac)_2$ as the structure-directing agent. The electrochemical tests reveal that the electrocatalytic performance of such 3D PdCu NCs are highly depended on their chemical compositions, where the composition-optimized $Pd_1Cu_{1.2}$ NCs displayed the highest EOR activity of 1790.8 mA mg^{-1} and 7.7 mA cm^{-2} for mass activity and specific activity, respectively. The incorporation of Cu is beneficial to facilitate the formation of OH species, improving the antipoisoning ability of catalysts. More importantly, the highly open 3D nanocage-like structure not only maximizes the atomic utilization of Pd, but also facilitates the mass/electron transfer. Both of which contribute to the excellent electrocatalytic activity and durability of 3D open-structured PdCu NCs toward EOR, and the excellent electrocatalytic performance make such 3D open-structured PdCu NCs a class of highly promising anode catalysts for EOR in DEFCs.

Acknowledgements

This work was supported by the National Natural Science Foundation of China (Grant No. 51873136), the Postgraduate Research & Practice Innovation Program of Jiangsu Province (KYCX18_2499), the project of Scientific and Technologic Infrastructure of Suzhou (SZS201708), the Priority Academic Program Development of Jiangsu Higher Education Institutions (PAPD).

Appendix A. Supplementary material

Supplementary data to this article can be found online at https://doi.org/10.1016/j.jcis.2019.07.092.

References

[1] R. Jiang, D.T. Tran, J.P. McClure, D. Chu, A class of (Pd–Ni–P) electrocatalysts for the ethanol oxidation reaction in alkaline media, ACS Catal. 4 (8) (2014) 2577–2586.
[2] A. Kowal, M. Li, M. Shao, K. Sasaki, M.B. Vukmirovic, J. Zhang, N.S. Marinkovic, P. Liu, A.I. Frenkel, R.R. Adzic, Ternary Pt/Rh/SnO_2 electrocatalysts for oxidizing ethanol to CO_2, Nat. Mater. 8 (4) (2009) 325–330.
[3] S. Guo, S. Dong, E. Wang, Pt/Pd bimetallic nanotubes with petal-like surfaces for enhanced catalytic activity and stability towards ethanol electrooxidation, Energy Environ. Sci. 3 (9) (2010) 1307.
[4] C. Hu, H. Cheng, Y. Zhao, Y. Hu, Y. Liu, L. Dai, L. Qu, Newly-designed complex ternary Pt/PdCu nanoboxes anchored on three-dimensional graphene framework for highly efficient ethanol oxidation, Adv. Mater. 24 (40) (2012) 5493–5498.
[5] Y. Shen, B. Gong, K. Xiao, L. Wang, In situ assembly of ultrathin PtRh nanowires to graphene nanosheets as highly efficient electrocatalysts for the oxidation of ethanol, ACS Appl. Mater. Interfaces 9 (4) (2017) 3535–3543.
[6] J. Yang, Y. Xie, R. Wang, B. Jiang, C. Tian, G. Mu, J. Yin, B. Wang, H. Fu, Synergistic effect of tungsten carbide and palladium on graphene for promoted ethanol electrooxidation, ACS Appl. Mater. Interfaces 5 (14) (2013) 6571–6579.
[7] F. Colmati, G. Tremiliosi-Filho, E.R. Gonzalez, A. Berna, E. Herrero, J.M. Feliu, The role of the steps in the cleavage of the C-C bond during ethanol oxidation on platinum electrodes, Phys. Chem. Chem. Phys.: PCCP 11 (40) (2009) 9114–9123.
[8] D. Chen, P. Sun, H. Liu, J. Yang, Bimetallic Cu–Pd alloy multipods and their highly electrocatalytic performance for formic acid oxidation and oxygen reduction, J. Mater. Chem. A 5 (9) (2017) 4421–4429.
[9] H. Xu, P. Song, C. Fernandez, J. Wang, M. Zhu, Y. Shiraishi, Y. Du, Sophisticated construction of binary PdPb Alloy nanocubes as robust electrocatalysts toward ethylene glycol and glycerol oxidation, ACS Appl. Mater. Interfaces 10 (15) (2018) 12659–12665.
[10] L. Bu, C. Tang, Q. Shao, X. Zhu, X. Huang, Three-Dimensional Pd_3Pb nanosheet assemblies: High-performance Non-Pt electrocatalysts for bifunctional fuel cell reactions, ACS Catal. 8 (5) (2018) 4569–4575.
[11] N. Benipal, J. Qi, Q. Liu, W. Li, Carbon nanotube supported PdAg nanoparticles for electrocatalytic oxidation of glycerol in anion exchange membrane fuel cells, Appl. Catal. Environ. 210 (2017) 121–130.
[12] X. Yu, P.G. Pickup, Novel Pd–Pb/C bimetallic catalysts for direct formic acid fuel cells, J. Power Sources 192 (2) (2009) 279–284.
[13] L. Sun, B. Liao, X. Ren, Y. Li, P. Zhang, L. Deng, Y. Gao, Ternary PdNi-based nanocrystals supported on nitrogen-doped reduced graphene oxide as highly active electrocatalysts for the oxygen reduction reaction, Electrochim. Acta 235 (2017) 543–552.
[14] B. Yan, H. Xu, K. Zhang, S. Li, J. Wang, Y. Shi, Y. Du, Cu assisted synthesis of self-supported PdCu alloy nanowires with enhanced performances toward ethylene glycol electrooxidation, Appl. Surf. Sci. 434 (2018) 701–710.
[15] C. Wang, D.P. Chen, X. Sang, R.R. Unocic, S.E. Skrabalak, Size-dependent disorder-order transformation in the synthesis of monodisperse intermetallic PdCu nanocatalysts, ACS Nano 10 (6) (2016) 6345–6353.
[16] Z. Zhao, H. Liu, W. Gao, W. Xue, Z. Liu, J. Huang, X. Pan, Y. Huang, Surface-engineered PtNi-O nanostructure with record-high performance for electrocatalytic hydrogen evolution reaction, J. Am. Chem. Soc. 140 (29) (2018) 9046–9050.
[17] S.-H. Han, H.-M. Liu, P. Chen, J.-X. Jiang, Y. Chen, Porous Trimetallic PtRhCu cubic nanoboxes for ethanol electrooxidation, Adv. Energy Mater. 8 (2018) 1801326.
[18] J. Bai, D. Liu, J. Yang, Y. Chen, Nanocatalysts for electrocatalytic oxidation of ethanol, ChemSusChem 12 (2019) 2117–2132.
[19] X. Yang, L.T. Roling, M. Vara, A.O. Elnabawy, M. Zhao, Z.D. Hood, S. Bao, M. Mavrikakis, Y. Xia, Synthesis and characterization of Pt-Ag alloy nanocages with enhanced activity and durability toward oxygen reduction, Nano Lett. 16 (10) (2016) 6644–6649.
[20] L. Wang, Y. Yamauchi, Metallic nanocages: synthesis of bimetallic Pt-Pd hollow nanoparticles with dendritic shells by selective chemical etching, J. Am. Chem. Soc. 135 (45) (2013) 16762–16765.
[21] S. Wang, J. Nai, S. Yang, L. Guo, Synthesis of amorphous Ni−Zn double hydroxide nanocages with excellent electrocatalytic activity toward oxygen evolution reaction, ChemNanoMat 1 (5) (2015) 324–330.
[22] J. Kim, H. Jin, A. Oh, H. Baik, S.H. Joo, K. Lee, Synthesis of compositionally tunable, hollow mixed metal sulphide $Co_xNi_yS_z$ octahedral nanocages and their composition-dependent electrocatalytic activities for oxygen evolution reaction, Nanoscale 9 (40) (2017) 15397–15406.
[23] C. Hu, X. Zhai, Y. Zhao, K. Bian, J. Zhang, L. Qu, H. Zhang, H. Luo, Small-sized PdCu nanocapsules on 3D graphene for high-performance ethanol oxidation, Nanoscale 6 (5) (2014) 2768–2775.
[24] J. Xue, G. Han, W. Ye, Y. Sang, H. Li, P. Guo, X.S. Zhao, Structural regulation of $PdCu_2$ nanoparticles and their electrocatalytic performance for ethanol oxidation, ACS Appl. Mater. Interfaces 8 (50) (2016) 34497–34505.
[25] Z. Gu, Z. Xiong, F. Ren, S. Li, H. Xu, B. Yan, Y. Du, Flower-like PdCu catalyst with high electrocatalytic properties for ethylene glycol oxidation, J. Taiwan Inst. Chem. Eng. 83 (2018) 32–39.
[26] Y. Huang, Y. Guo, Y. Wang, J. Yao, Synthesis and performance of a novel PdCuPb/C nanocatalyst for ethanol electrooxidation in alkaline medium, Int. J. Hydrogen Energy 39 (9) (2014) 4274–4281.
[27] S. Fu, C. Zhu, J. Song, P. Zhang, M.H. Engelhard, H. Xia, D. Du, Y. Lin, Low Pt-content ternary PdCuPt nanodendrites: an efficient electrocatalyst for oxygen reduction reaction, Nanoscale 9 (3) (2017) 1279–1284.
[28] M. Iqbal, C. Li, J.H. Kim, S.M. Alshehri, T. Nakayama, Y. Yamauchi, Three-dimensional super-branched PdCu nanoarchitectures exposed on controlled crystal facets, Chemistry 23 (1) (2017) 51–56.

[29] K. Zhang, C. Wang, D. Bin, J. Wang, B. Yan, Y. Shiraishi, Y. Du, Fabrication of Pd/P nanoparticle networks with high activity for methanol oxidation, Catal. Sci. Technol. 6 (16) (2016) 6441–6447.
[30] J. Zhong, D. Bin, Y. Feng, K. Zhang, J. Wang, C. Wang, J. Guo, P. Yang, Y. Du, Synthesis and high electrocatalytic activity of Au-decorated Pd heterogeneous nanocube catalysts for ethanol electro-oxidation in alkaline media, Catal. Sci. Technol. 6 (14) (2016) 5397–5404.
[31] C. Wang, L. Zhang, H. Yang, J. Pan, J. Liu, C. Dotse, Y. Luan, R. Gao, C. Lin, J. Zhang, J.P. Kilcrease, X. Wen, S. Zou, J. Fang, High-Indexed Pt_3Ni alloy tetrahexahedral nanoframes evolved through preferential CO etching, Nano Lett. 17 (4) (2017) 2204–2210.
[32] L.-M. Lyu, Y.-C. Kao, D.A. Cullen, B.T. Sneed, Y.-C. Chuang, C.-H. Kuo, Spiny rhombic dodecahedral CuPt nanoframes with enhanced catalytic performance synthesized from Cu nanocube templates, Chem. Mater. 29 (13) (2017) 5681–5692.
[33] W. Ye, S. Kou, X. Guo, F. Xie, H. Sun, H. Lu, J. Yang, Controlled synthesis of bimetallic Pd-Rh nanoframes and nanoboxes with high catalytic performances, Nanoscale 7 (21) (2015) 9558–9562.
[34] F. Nosheen, Z.C. Zhang, J. Zhuang, X. Wang, One-pot fabrication of single-crystalline octahedral Pt-Cu nanoframes and their enhanced electrocatalytic activity, Nanoscale 5 (9) (2013) 3660–3663.
[35] K. Wang, R. Sriphathoorat, S. Luo, M. Tang, H. Du, P.K. Shen, Ultrathin PtCu hexapod nanocrystals with enhanced catalytic performance for electro-oxidation reactions, J. Mater. Chem. A 4 (2016) 13425–13430.
[36] L. Jin, H. Xu, C. Chen, T. Song, C. Wang, Y. Wang, H. Shang, Y. Du, Uniform PdCu coated Te nanowires as efficient catalysts for electrooxidation of ethylene glycol, J. Colloid Interface Sci. 540 (2019) 265–271.
[37] H. Shang, H. Xu, Q. Liu, Y. Du, PdCu alloy nanosheets-constructed 3D flowers: new highly sensitive materials for H_2S detection, Sens. Actuat. B: Chem. 289 (2019) 260–268.
[38] X. Guo, H. Shang, J. Guo, H. Xu, Y. Du, Ultrafine two-dimensional alloyed PdCu nanosheets-constructed three-dimensional nanoflowers enable efficient ethylene glycol electrooxidation, Appl. Surf. Sci. 481 (2019) 1532–1537.
[39] G.-T. Fu, B.-Y. Xia, R.-G. Ma, Y. Chen, Y.-W. Tang, J.-M. Lee, Trimetallic PtAgCu@PtCu core@shell concave nanooctahedrons with enhanced activity for formic acid oxidation reaction, Nano Energy 12 (2015) 824–832.